



# “Off-on” fluorescence probe based on green emissive carbon dots for the determination of $\text{Cu}^{2+}$ ions and glyphosate and development of a smart sensing film for vegetable packaging

Jiajie Wu<sup>1</sup> · Xiaoyong Chen<sup>1,2</sup> · Zeyu Zhang<sup>1</sup> · Jiamin Zhang<sup>1</sup>

Received: 26 October 2021 / Accepted: 21 February 2022 / Published online: 3 March 2022  
© The Author(s), under exclusive licence to Springer-Verlag GmbH Austria, part of Springer Nature 2022

## Abstract

An ultra-sensitive glyphosate nanosensor, based on carbon dots (CDs), was successfully developed with excellent long-wavelength emission (530 nm), a high quantum yield (41.3%), and an impressive detection limit ( $0.8 \text{ ng}\cdot\text{mL}^{-1}$ ). This is the lowest value for glyphosate detection achieved by CD-based fluorescence analysis. The sensor was derived from a separate precursor, 1,4-dihydroxyanthraquinone, and was based on the “off-on” fluorescence analysis, where  $\text{Cu}^{2+}$  acts as a dynamic quencher and glyphosate as a fluorescence restorer (excitation wavelength 460 nm). Trace detection of glyphosate is possible with a wide detection range of  $50\text{--}1300 \text{ ng}\cdot\text{mL}^{-1}$  and spiked recoveries between 93.3 and 110.0%. Exploration in depth confirmed that (1) the fluorescence of CDs was derived from the carbon core, (2) the large  $\text{sp}^2$  conjugated domain consisting of graphitic carbon and nitrogen contributed to the long-wavelength emission, and (3) CDs had an impressive binding interaction with  $\text{Cu}^{2+}$ , which endow high sensitivity to glyphosate detection. The nanosensor has also be used as a dual-mode visual sensor and a smart sensing membrane that can identify glyphosate on the surface of vegetables, thus showing good practical applicability.

**Keywords** Fluorescent · Carbon dots · Nanosensor ·  $\text{Cu}^{2+}$  and glyphosate detection · Smart packaging

## Introduction

Ultra-sensitive detection is important for biochemical analysis [1, 2], food safety [3, 4], health diagnosis [5, 6], and environmental protection [7, 8]. These include the early recognition of viruses (e.g., SARS-CoV-2) that cause illnesses, the powerful detection of negligible contents of deadly toxins and poisons (e.g., aflatoxin, botulinum toxin, and biological hallucinogens in certain poisonous mushrooms), and the sensitive perception of trace elements with increasingly serious implications and pesticide residues in the environment [9]. Glyphosate (GP) is a widely used herbicide; its continuous use in agricultural production has led to its persistent

presence in the soil, which has serious effects on biological health and causes environmental degradation. Currently, GP detection technologies mainly include gas chromatography, high-performance liquid chromatography, ion chromatography, gas chromatography tandem mass spectrometry, high-performance liquid chromatography tandem mass spectrometry, and immunoassays [10, 11]. These methods have high detection efficiency and sensitivity; however, the detection process is cumbersome and costly.

With good biocompatibility [12, 13], low toxicity [14, 15], and low preparation cost, carbon dots (CDs) have a wide range of applications for detection [16, 17], catalysis, and biochemical analysis [18, 19]. CD-based detection systems have been widely used for the sensing of metal ions and related anions [19–21], and have also been studied for applications in pesticide residue analysis [22–24]. The screening for GP using CDs has been reported in previous studies. Guerrero-Esteban et al. [25] published an impressive value on GP detection value of  $8.66 \text{ pg}\cdot\text{mL}^{-1}$ , which was the lowest detection limit to the best of our knowledge. However, their results were derived from a CD-based electrochemiluminescence immunosensor, which created obstacles for

✉ Xiaoyong Chen  
chenxiaoyong@nuc.edu.cn

<sup>1</sup> The School of Chemical Engineering and Technology, North University of China, Taiyuan 030051, China

<sup>2</sup> The Key Laboratory of Instrumentation Science & Dynamic Measurement, Ministry of Education, North University of China, Taiyuan 030051, China

portable practice through electrification, control modules, and precious immunosensor. The detection techniques of GP, with relatively high cost-efficiency, such as fluorescence detection have been reported. Bera et al. [26], Jiménez-López et al. [27] and Wang et al. [28] explored the fluorescent detection of GP using intertwining CDs-X where X = CdTe quantum dots, X = Ag nanoparticles, and X = Ag nanoparticles. These studies all reported high sensitivity, up to ng level in detection limits; however, CdTe and Ag are not eco-friendly.

New toxicity-free solutions have been proposed. Yuan et al. [29] developed a GP detection, based on blue-emitting CDs from citric acid and tris(hydroxymethyl)methylaminomethane with a detection limit of  $0.6 \mu\text{mol}\cdot\text{L}^{-1}$ , which was a relatively low sensitivity and did not require hazardous heavy metals. Wang et al. [30] improved the sensing sensitivity to  $16 \text{ ng}\cdot\text{mL}^{-1}$ , using blue fluorescent CDs obtained from thiourea and diethylene glycol systems. Notably, Wang et al. [31] and Hou et al. [32], achieved a resolution of  $8.0 \text{ ng}\cdot\text{mL}^{-1}$  through a precious immune-related CD-based detection GP and a resolution of  $8.65 \text{ ng}\cdot\text{mL}^{-1}$  through a sophora-japonica-leaves-based CD. These studies avoided the use of environmentally hazardous species; however, the end products were derived from multiple precursors, resulting in heterogeneities in the carbon core, which broadened the CD emission spectrum and led to poor consistency in CD production. In addition, these CDs exhibit blue fluorescence, which limited biological applications because of photonic toxicity and autofluorescence interference from biological tissues. Consequently, single precursor-based, long-wavelength emissive CDs for GP detection are in high demand.

In this study, a CD/ $\text{Cu}^{2+}$  fluorescent nanoprobe was constructed for the ultra-sensitive determination of GP based on the fluorescence of CDs that are quenched by the dynamic and static action of  $\text{Cu}^{2+}$ . The concentration of GP showed good linearity with  $F/F_0$  in the range of  $50\text{--}300 \text{ ng}\cdot\text{mL}^{-1}$  with a maximum detection limit of  $0.8 \text{ ng}\cdot\text{mL}^{-1}$  ( $5 \text{ nM}$ ), which was an order of magnitude lower than existing fluorescent CD-based methods for the detection of GP residues. Detailed structural and property analyses were conducted, which confirmed that these CDs were excitation-independent and their luminescence originated from the carbon core with a large  $\text{sp}^2$  conjugation domain from graphitic carbon and nitrogen. To further demonstrate the engineering value of the developed CDs, we developed a conceptual smart package for the self-reporting of GP residues on vegetables. The results provide a new solution for ultra-sensitive GP detection and self-reporting smart kits, and further contribute to safer food and the environment.

## Experimental section

### Materials

1,4-dihydroxyanthraquinone,  $\text{CoCl}_2$ ,  $\text{NaCl}$ ,  $\text{CuSO}_4$ ,  $\text{ZnCl}_2$ ,  $\text{MgCl}_2$ ,  $\text{HgCl}_2$ ,  $\text{Ni}(\text{NO}_3)_2$ ,  $\text{MnCl}_2$ ,  $\text{NH}_4\text{Cl}$ ,  $\text{Al}_2(\text{SO}_4)_3$ ,  $\text{CoCl}_2$ , formamide, ethanol, dichloromethane (DCM), glyphosate (GP), trichlorfon, 1-naphthofen, carbaryl, carbendazim, polyvinyl alcohol (PVA), acrylamide, ammonium persulphate etc, and all of the reagents were purchased from Shanghai Macklin Biochemical Co., Ltd (<http://www.macklin.cn/>) and were used without further treatment.

### Synthesis of green fluorescent CDs

Green fluorescent carbon dots (G-CD) were synthesized by a solvent thermal method using 1,4-dihydroxyanthraquinone as a precursor. In general, 5 mg of 1,4-dihydroxyanthraquinone was dissolved in 10 mL of formamide solvent, sonicated for 5 min, and then transferred into a 25 mL stainless steel reactor with polytetrafluoroethylene liner, reacting at a constant temperature oven at  $180 \text{ }^\circ\text{C}$  for 8 h. After the reactor had cooled to room temperature ( $25 \text{ }^\circ\text{C}$ ), the purification was carried out by extraction, using DCM as an extractant for 3 times. After extraction, the resulting solution was washed 5 times with distilled water to remove the impurities. Then, the resulting solution was dried in an oven at  $60 \text{ }^\circ\text{C}$  to remove the solvent, resulting in a brownish-yellow powder.

### Physical characterization

The dimensions of the G-CD were measured using a transmission electron microscope (TEM, JEM2100F <https://www.jeol.co.jp/>). The chemical composition and bonding structure of the G-CD were determined by X-ray photoelectron spectroscopy (XPS, Thermo Fisher Escalab 250Xi <https://www.jp.xpssimplified.com>); the fluorescence quantum yield (QY) of the G-CD solutions was determined by a fluorescence spectrometer (Edinburgh FLS1000 <https://www.edinst.com>), and the Raman spectra by a Raman spectrometer (<https://www.jp.xpssimplified.com>), the Fourier transform infrared spectra (FTIR) on a Nicolet 5700 IR spectrometer (<https://www.acap.net.au/>), and the fluorescence spectra and UV absorption spectra by a fluorescence spectrometer F-7000 (Hitachi, Japan <https://www.hitachi.co.jp>) and a Volmer (Lambda 35), respectively. (Please refer to ESM for experimental data results.)

## Fluorescence assay of Cu<sup>2+</sup> and GP

The detection of Cu<sup>2+</sup> by G-CD was performed at room temperature (25 °C): taking 3 mL of ethanolic dispersion of G-CD at 0.5 mg·mL<sup>-1</sup>, then adding different concentrations of Cu<sup>2+</sup> standards, stirring and mixing the resultant solution thoroughly, and measuring and recording the fluorescence spectrum of the dispersion after 1 min. (Number of experiments  $n = 5$ .)

The detection of GP was performed at room temperature: 9.6 µg of Cu<sup>2+</sup> standard was added to 3 mL of an ethanolic dispersion of 0.5 mg·mL<sup>-1</sup> and stirred until the fluorescence of the dispersion was completely quenched. The standard concentration of GP was dropped into the above-mentioned dispersion, stirred and mixed thoroughly, and after 1 min the fluorescence spectrum of the dispersion was measured and recorded. All assays were performed under identical conditions. (Number of experiments  $n = 5$ .)

## Applications in real samples

Different concentrations of GP (0, 1, 3, 5, and 10 µg) were added to five 100 g portions of different cucumber and lettuce parts. Thereafter, they were crushed in a juicer, and 100 mL each of water and DCM were added. After sonication for 30 min, the supernatant was centrifuged at 8000 rpm for 20 min, and the supernatant was concentrated to 5 mL. The detection method was similar to that described in “Materials.” (Number of experiments  $n = 5$ .)

## Result and discussion

### Choice of materials

1,4-dihydroxyanthraquinone has abundant ‘-OH’ and ‘=O’ groups, and a large conjugated structure can be formed by the solvent thermal method, thus realizing the preparation of long-wavelength emitting carbon dots. Moreover, it has high antitumor activity, is a bio-friendly raw material, and is inexpensive. Polyvinyl alcohol (PVA) is a biodegradable polymer material that does not pollute the environment and is inexpensive. Its oil resistance, solvent resistance, and gas barrier properties are outstanding, and it has unique advantages in food and pharmaceutical packaging. The polyacrylamide (PAM) structural unit contains an amide group, which is easy to form hydrogen bonds, so that it has good water solubility and high chemical activity, and can form hydrogen bonds with the amino group of G-CD.

## Detection of Cu<sup>2+</sup> and GP

“Off” and “off/on” sensors were prepared to detect Cu<sup>2+</sup> and GP, respectively, based on the ability of Cu<sup>2+</sup> to quench the fluorescence of G-CD and the subsequent restoration of G-CD fluorescence by GP.

Using a syringe needle, 0.01 M Cu<sup>2+</sup> was added to the ethanol dispersion of G-CD. The solution gradually turned from green to yellow in color, with the addition of Cu<sup>2+</sup>, and the fluorescence of the solution changed from green to blue (at 365nm UV light). Figure 1a and 1b show that there was a good linear relationship between  $F/F_0$  and Cu<sup>2+</sup> concentration when the concentration of Cu<sup>2+</sup> is in the range of 50–800 ng·mL<sup>-1</sup>, with a linear equation of  $y = -0.0113x + 1.0716$  ( $R^2 = 0.993$ ). The limit of detection (LOD) was determined by  $3\sigma/K$ , where  $\sigma$  is the standard deviation of the lowest signal ( $n = 5$ ) and  $K$  is the slope of the linear calibration plot. The experimental results indicated that the detection limit of Cu<sup>2+</sup> is 22.65 nM.

It was found that GP could restore the fluorescence of G-CD that was quenched by Cu<sup>2+</sup>. Based on the experimental results of the previous steps, 9.6 µg of Cu<sup>2+</sup> was chosen to completely quench the G-CD.

As shown in Fig. 1c, the fluorescence of the G-CD was quenched by adding 9.6 µg of Cu<sup>2+</sup> with a syringe needle at an excitation wavelength of 460 nm. Under the same experimental conditions, a standard sample of 0.01 M GP was added to the quenched G-CD dispersion and the fluorescence spectrum of the dispersion was measured and recorded. When 15.21 µg of GP was added, the fluorescence of the G-CD was almost restored to its original intensity, with a recovery rate of 98%, while the color of the solution gradually changed from yellow to green. When the concentration of GP was in the range of 50–1300 ng·mL<sup>-1</sup>,  $F/F_0$  and the concentration of GP had a good linear relationship (Fig. 1d), and the linear equation was  $y = 0.1961x + 0.0487$  ( $R^2 = 0.993$ ). Therefore, the LOD of the GP was 0.8 ng·mL<sup>-1</sup> (5 nM), which was significantly lower than the existing minimum detection limit of 2 ng·mL<sup>-1</sup> for fluorescence analysis.

To understand this impressive LOD, the binding constants of the G-CD/Cu<sup>2+</sup> and Hou et al.’s [32] CD/Fe<sup>3+</sup> system were calculated and compared (Table 1). The formula was as follows:  $\log \frac{F_0 - F}{F} = \log K_a + n \log [Q]$ .  $F_0$  is the fluorescence intensity without a quencher,  $F$  is the fluorescence intensity with the addition of a quencher,  $K_a$  is the corresponding binding constant,  $Q$  is the concentration of the quencher substance, and  $n$  is the number of binding sites. It was found that the G-CD/Cu<sup>2+</sup> system had a significantly larger binding constant and binding numbers than Hou et al.’s [32] CD/Fe<sup>3+</sup> system and Tafreshi et al. [33]. We believe that because G-CD and Cu<sup>2+</sup> are bound by strong binding forces, they can bond well to Cu<sup>2+</sup> even in extremely dilute Cu<sup>2+</sup> solutions. Therefore, the G-CD/Cu<sup>2+</sup> system is more sensitive

**Fig. 1** Detection of  $\text{Cu}^{2+}$  by G-CD at 460 nm. **a** Fluorescence spectra of solutions with increasing  $\text{Cu}^{2+}$  concentration. **b** Linear relationship between  $\text{Cu}^{2+}$  and  $F/F_0$ . Detection of GP with G-CD. **c** Fluorescence spectrum of the solution with increasing GP concentration. **d** Linear relationship between GP concentration and  $F/F_0$

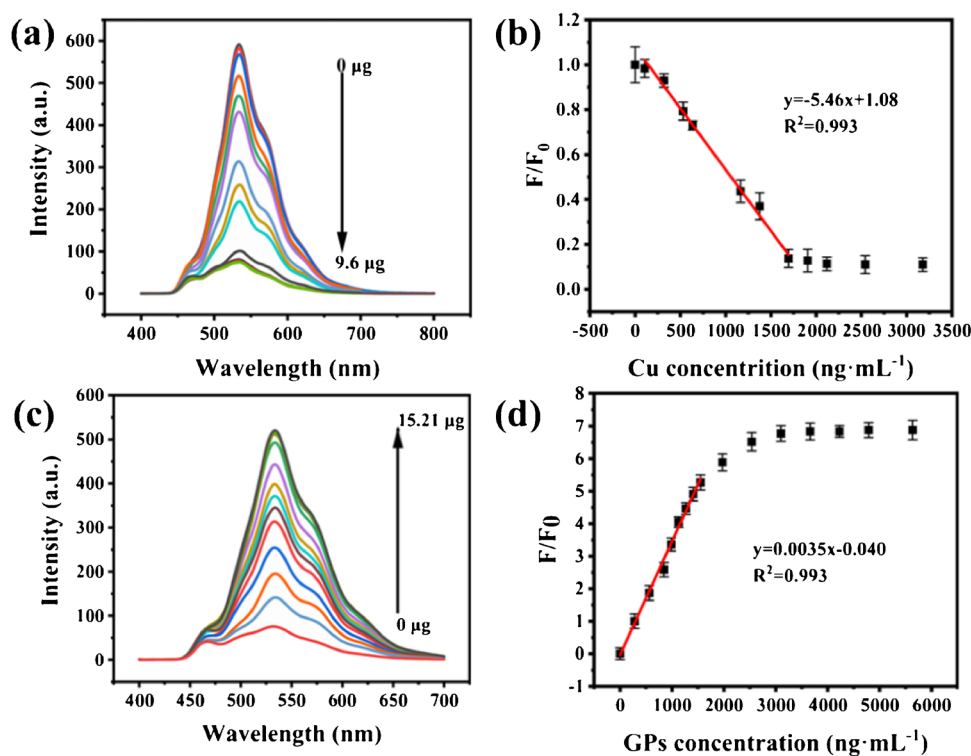


**Table 1** Comparison of the GP detection limit of the sensor with previously reported results for other sensors

Sensing probe	Linear range ( $\mu\text{g}\cdot\text{mL}^{-1}$ )	LOD ( $\text{ng}\cdot\text{mL}^{-1}$ )	$K_a$	Reference
CD/AgNPs	0.025–2.5	12	-	[28]
CD/ $\text{Fe}^{3+}$	0.1–16	8.75	1800	[32]
IgG-CDs	0.01–80	8	-	[31]
CDs	3.38–338.14	101.4	-	[29]
CD/ $\text{Cu}^{2+}$	0.03–10	16	-	[30]
CDs	0.01–0.8	2	$3 \times 10^5$	[33]
CD/ $\text{Cu}^{2+}$	0.05–1.3	0.8	$3 \times 10^8$	This work

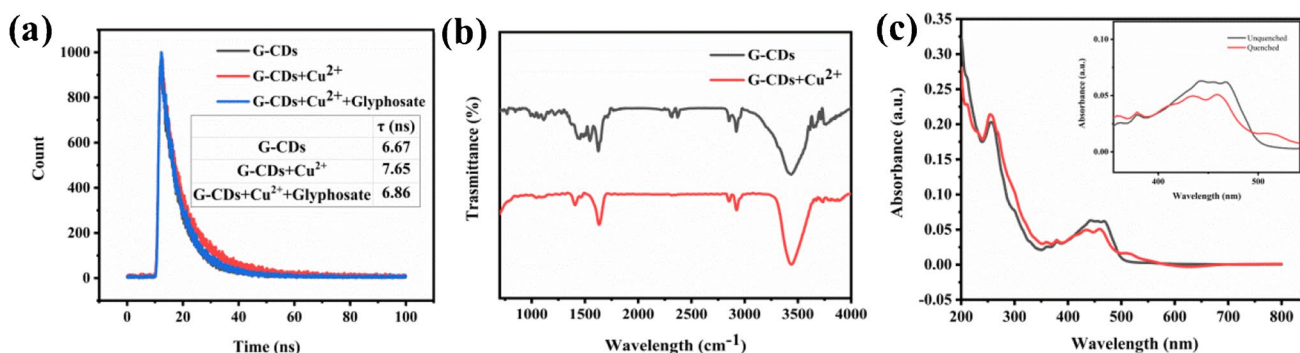
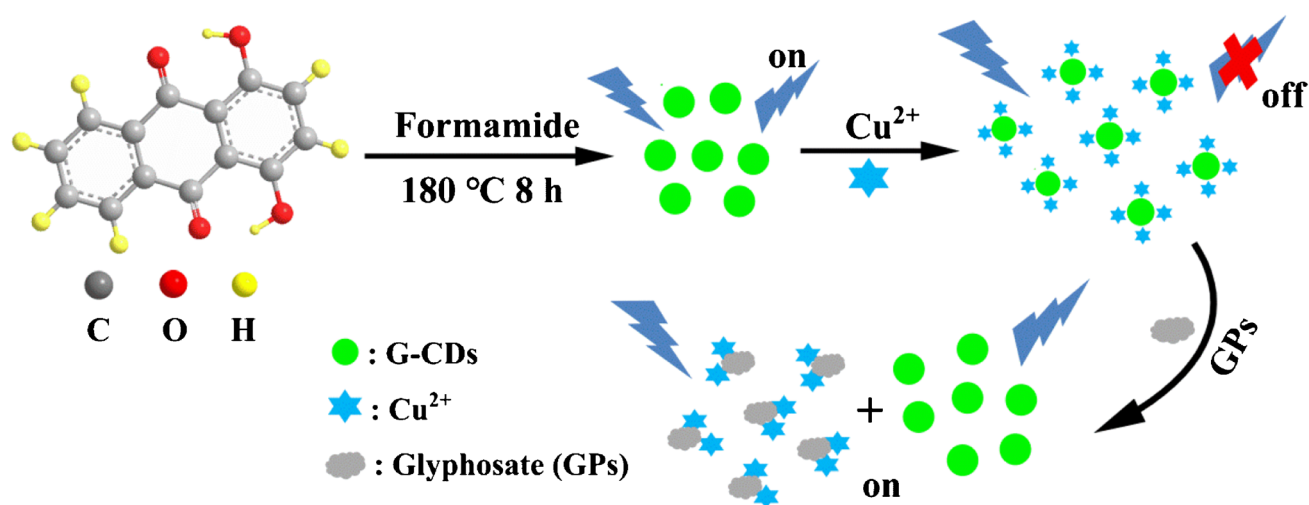


**Fig. 2** **a** Fluorescence lifetimes of G-CD, G-CD+ $\text{Cu}^{2+}$ , and G-CD+ $\text{Cu}^{2+}$ +GP. **b** FTIR spectra of G-CD and G-CD+ $\text{Cu}^{2+}$ . **c** UV-Vis absorption spectra of G-CD and G-CD after quenching



**Scheme 1** Synthetic methods for carbon dots and detection mechanisms for glyphosate

to fluorescence switching, resulting in the relatively high sensitivity of our nanosensor.

To understand the detection mechanism of G-CD on Cu<sup>2+</sup> and GP, a fluorescence lifetime test was performed on G-CD and its mixtures (Fig. 2a). The fluorescence lifetime of the G-CD was 6.67 ns, while the fluorescence lifetime of the G-CD/Cu<sup>2+</sup> system was 7.65 ns. The fluorescence lifetime variation indicated that Cu<sup>2+</sup> might quench the fluorescence of G-CD through dynamic effects. To further understand the mechanism of quenching, UV-vis absorption spectra before and after G-CD fluorescence quenching were measured. A strong absorption peak in the range of 442–470 nm appeared in the G-CD solution and blue-shifted to 430–459 nm after the addition of Cu<sup>2+</sup>, meaning that a new complex was formed due to possible complexation between Cu<sup>2+</sup>, –NH<sub>2</sub>, and –OH on the G-CD surface (Fig. 2c). Further observations were observed in the FTIR spectra. As shown in Fig. 2b, the C–N peak at 1433 cm<sup>-1</sup> was notably reduced and the –NH<sub>2</sub> peak at 3315 cm<sup>-1</sup> disappeared, indicating that Cu<sup>2+</sup> complexed with –NH<sub>2</sub>. From these spectrographic pieces of evidence and fluorescence lifetimes, it could be inferred that the quenching might be a combination of static and dynamic. When GP was gradually added, the fluorescence intensity of the solution gradually recovered, and the fluorescence lifetime of G-CD + Cu<sup>2+</sup> + GP was 6.86 ns, which was not significantly changed compared with the initial fluorescence lifetime of G-CD (Fig. 2a). This resulted from the stronger interaction between GP and Cu<sup>2+</sup> than between G-CD and Cu<sup>2+</sup>; thus, Cu<sup>2+</sup> could be completely stripped from the G-CD/Cu<sup>2+</sup> system. In addition, the fluorescence of G-CD was restored because of the GP structure (–COOH and –NH<sub>2</sub>) and the high binding constants of Cu<sup>2+</sup> in GP. The Stern-Volmer equation for dynamic quenching is  $F_0/F = 1 + K_d[Q]$  and the equation for

static quenching is  $F_0/F = 1 + K_s[Q]$ .  $F_0$  is the fluorescence intensity before quenching,  $F$  is the fluorescence intensity after quenching,  $K_d$  is the dynamic quenching constant,  $K_s$  is the static quenching constant, and  $Q$  is the concentration of the quencher. The Stern-Volmer plot is a linear line if the quenching mechanism of carbon sites is static or dynamic. But the Stern-Volmer diagram is curved and conforms to the modified equation  $F_0/F = (1 + K_d[Q])(1 + K_s[Q])$ , the quenching mechanism of G-CD is a combination of dynamic and static quenching (Fig. S6). The mechanism is shown in Scheme 1.

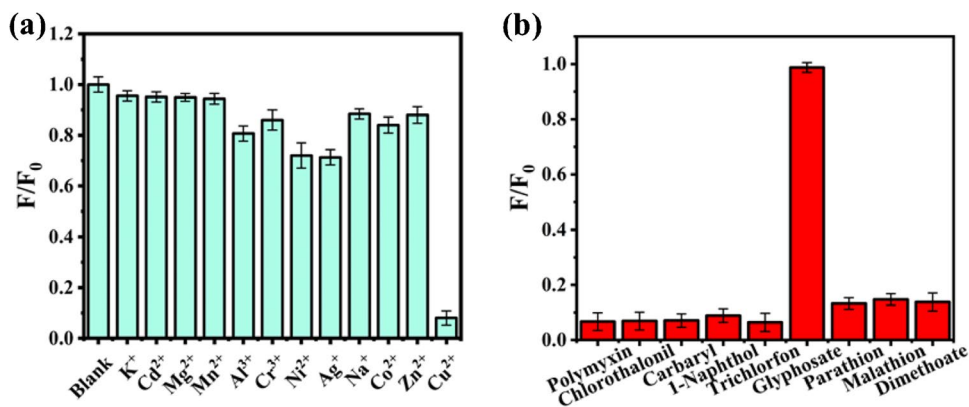
Hou et al. [34], Hou et al. [32], Tafreshi et al. [33], and Yuan et al. [29] used their fluorescent probes for the detection of GP (Table 1). Although their fluorescent probes had a wide linear detection range and high detection limit, they were not portable. In contrast, we prepared fluorescent films based on synthetic G-CD that have better portability while maintaining excellent detection.

### Selectivity and interference studies

The ion selectivity of G-CD was tested in the presence of K<sup>+</sup>, Cd<sup>2+</sup>, Mg<sup>2+</sup>, Mn<sup>2+</sup>, Al<sup>3+</sup>, Cr<sup>3+</sup>, Ni<sup>2+</sup>, Ag<sup>+</sup>, Na<sup>+</sup>, Co<sup>2+</sup>, Zn<sup>2+</sup>, and Cu<sup>2+</sup> ions at quenching concentrations significantly higher than Cu<sup>2+</sup> (64 μg), and the test results showed that G-CD had good selectivity (Fig. 3a). Subsequently, tests on the selectivity of the G-CD were executed on pesticides. Nine pesticides (carbendazim, trichlorfon, clothianidin, carbaryl, 1-naphthol and GP, parathion, dimethoate malathion, and parathion) were selected and tested under the same conditions. The experimental results showed that G-CD/Cu<sup>2+</sup> had the most sensitive response to GP, while the response to other non-organophosphorus and organophosphorus pesticides reduced and was less



**Fig. 3** G-CD selectivity test for **a** ions and **b** pesticides at an excitation wavelength of 460 nm



sensitive (Fig. 3b). This resulted from  $Cu^{2+}$  having more binding sites with GP than other non-organophosphorus and organophosphorus pesticides, which easily generated stable complexes and had a stronger binding ability compared with other pesticides. The sensor has good reversibility and reusability. As shown in Fig. S7, 9.6  $\mu\text{g}$  of  $Cu^{2+}$  standard was added to 3 mL of 0.5  $\text{mg}\cdot\text{mL}^{-1}$  GP ethanol dispersion. And stirring until the fluorescence of the dispersion was completely quenched. Then, the standard concentration of GP was dropped into the dispersion, stirring until the fluorescence of the dispersion was completely recovered. The above experimental procedure was repeated 6 times. The high sensitivity of G-CD/ $Cu^{2+}$  for the detection of GP was still observed after 6 times of use (Fig. S7). It indicates that our fluorescent sensor can be used repeatedly.

When the G-CD are dispersed in an ethanol medium, the addition of trace amounts of water (20  $\mu\text{L}$ ) does not affect the fluorescence intensity of the G-CD. In contrast, the fluorescence intensity of the solution was significantly reduced when a small amount of aqueous  $Cu^{2+}$  solution (20  $\mu\text{L}$ ) was added to the dispersion. The ethanol solution of 0.01 M  $Cu^{2+}$  was added dropwise to the ethanol dispersion of G-CD, and the same result was obtained as that of an aqueous solution of  $Cu^{2+}$  added to the ethanol dispersion of G-CD. In two cases, the binding constant of  $Cu^{2+}$  was calculated to be  $3\times 10^8$ , quantitatively demonstrated the good affinity between G-CD and  $Cu^{2+}$  (Fig. S8).

After the G-CD fluorescence was quenched by  $Fe^{3+}$ , it required the addition of 1 mg of GP to recover, which was 100 times the amount needed to be added after  $Cu^{2+}$  quenching. As shown in Fig. S4, after storing the G-CD at room temperature (25  $^{\circ}\text{C}$ ) for 120 days, they still have good luminescence performance and the fluorescence intensity is basically unchanged compared with that before. It shows that our sensors have good stability. As shown in Fig. S5, the presence of other ions did not affect the detection of GP. The experimental results show that G-CD/ $Cu^{2+}$  has good selectivity.

### Detection of $Cu^{2+}$ and GP in real samples

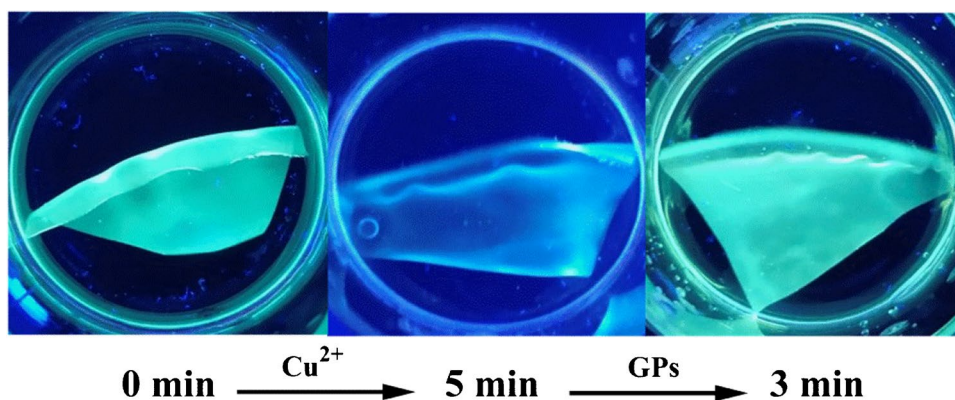
The fluorescence of G-CD was first quenched by  $Cu^{2+}$ , and thereafter the unlabeled cucumber solution to be tested was added. A 5  $\mu\text{L}$  sample of the solution was measured and 0.01  $\text{mol}\cdot\text{L}^{-1}$  of GP added to it until the fluorescence of the solution was restored (Fig. S6). The residual amount of GP in cucumber was calculated as 0.084  $\text{mg}\cdot\text{kg}^{-1}$ , which was significantly lower than the maximum residual amount of 1  $\text{mg}\cdot\text{kg}^{-1}$  (GB 2763-2021), indicating that our fluorescent probe was equally significant for the detection of real samples.

Based on the above experimental results, the probe was used to detect  $Cu^{2+}$  in water and GP residues in vegetables (Table 2). As shown in Table 2, the recoveries of these samples ranged from 93.3 to 110.0%; the results indicated that the constructed nanosensor was sensitive and reliable for the detection of  $Cu^{2+}$  and GP in real samples.

**Table 2** Spiked determination and detection of GP in cucumber and lettuce samples of  $Cu^{2+}$  in water

Sample	Added ( $\mu\text{g}$ )	Measured ( $\mu\text{g}$ )	Recovery	RSD ( $n=5$ )
Tap water	0	0	-	-
	10.0	9.8	98.0%	3.3
	20.0	18.8	94.0%	2.8
	30.0	31.2	104.0%	2.7
	50.0	48.2	96.4%	3.5
Cucumber	0.0	0	-	-
	1	1.1	110.0%	1.7
	3	2.8	93.3%	2.3
	5	4.7	94%	2.1
	10	10.3	103.0%	3.2
Lettuce	0	0	-	-
	1	0.97	97.0%	3.1
	3	3.1	103.3%	2.3
	5	4.8	96.0%	2.7
	10	10.2	102.0%	2.5

**Fig. 4** Fluorescence quenching of G-CD films by 365 nm UV light and its recovery



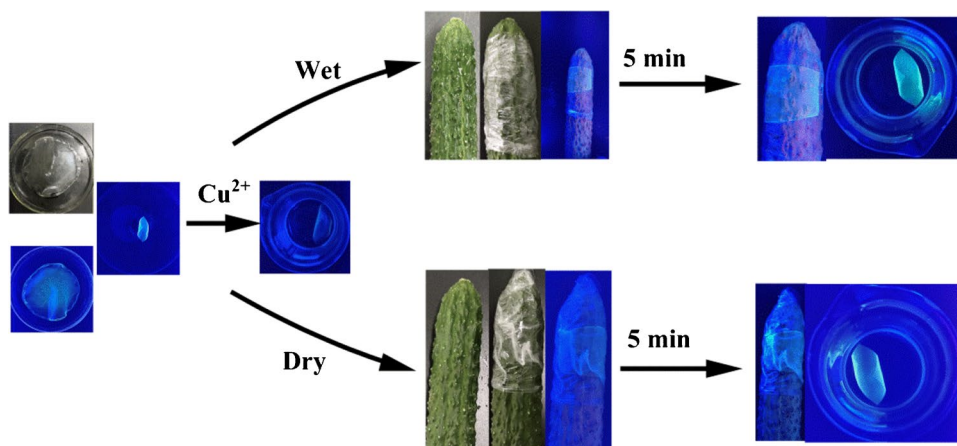
### GP portable sensors and smart packaging applications

In addition, G-CD fluorescent films were prepared using in situ polymerization. As shown in Fig. 4, the prepared fluorescent films still exhibited good luminescence properties. Consequently, a fluorometric and colorimetric dual-mode, fluorescent film-based array was developed for inspecting  $\text{Cu}^{2+}$  and GP, based on  $\text{Cu}^{2+}$  induction the color and fluorescence intensity changes in G-CD while GP inversely transforms the changes. The dual-mode sensing results are shown in Figs. 4 and 5. The visual results are intuitive and convenient for everyday applications that require portability and convenience. (For the preparation of fluorescent films, please refer to ESM.)

The prepared fluorescent films exhibited a rapid and strong response to  $\text{Cu}^{2+}$  and GP. This indicated the potential of G-CD-based films in smart applications. These films were used to detect the surface residues of GP in vegetables such as cucumbers. First, 0.5 mL of  $0.01 \text{ mol}\cdot\text{L}^{-1}$   $\text{Cu}^{2+}$  was diluted to 20 mL, and thereafter the G-CD film was placed and its fluorescence quenched completely.

Thereafter, 0.5 mL of  $0.01 \text{ mol}\cdot\text{L}^{-1}$  GP was diluted to 50 mL, sprayed on the surface of a cucumber, and the quenched G-CD film placed on top and wrapped with cling film. After approximately 5 min, the fluorescence of the film turned from blue to green in color under a 365 nm UV lamp; the fluorescence intensity recovered to its original intensity. Thereafter, the same amount of GP was sprayed on the surface of the cucumber, and dried with a hair dryer, and then the quenched G-CD film was placed on it and wrapped with plastic wrap. According to Xu et al. [35], we speculate that because the film contains abundant functional groups, the GP on the surface of cucumber penetrates the surface of G-CD through adsorption, causing the monitoring reaction of G-CD. Thus, GP gradually entered the film, and the fluorescence of the film recovered after approximately 5 min. Since G-CD is encapsulated in a thin film, it reduces the sensitivity of the sensor. The visual detection limit of the fluorescent film was  $10 \mu\text{M}$ . The experimental results demonstrated that the G-CD fluorescent film had a sensitive response to GP, regardless of whether the surface of the cucumber was dry or wet, which was the desired result, thus indicating that the film had great potential for application in smart packaging.

**Fig. 5** Images of G-CD fluorescent film for detecting GP on the surface of wet and dry cucumber



## Conclusion

The CDs synthesized in this study had high fluorescence quantum yields (41.3%) and photochemical stability. This study achieved ultra-sensitive fluorescence detection of GP based on long-wavelength CDs (530 nm) with excellent selectivity and interference resistance. The simultaneous fluorescence intensity and macroscopic color change when detecting  $\text{Cu}^{2+}$  and GP, allowed for the visualization of the detection capability a fluorescent and colorimetric dual-mode sensing technique. The CD nanosensor was also used to detect real samples, such as cucumber and lettuce, demonstrating excellent capabilities for practical applications. However, the detection limit of fluorescent films of GP was 10  $\mu\text{M}$ ; therefore, the sensitive detection of CD fluorescent films requires further investigation.

**Supplementary Information** The online version contains supplementary material available at <https://doi.org/10.1007/s00604-022-05241-5>.

**Funding** This work was supported by the Natural Science Foundation of Shanxi Province China (201901D111140), the National Science Fund for Distinguished Young Scholars under Grant No. 51425505, the National Natural Science Foundation of China (Youth Project) under Grant No. 51505435, and China Postdoctoral Science Foundation under Grant No. 2014M551061.

## Declarations

**Conflict of interest** The authors declare no competing interests.

## References

- Wang Q, Yin Q, Fan Y, Zhang L, Xu Y, Hu O, Guo X, Shi Q, Fu H, She Y (2019) Double quantum dots-nanoporphyrin fluorescence-visualized paper-based sensors for detecting organophosphorus pesticides. *Talanta* 199:46–53. <https://doi.org/10.1016/j.talanta.2019.02.023>
- Wu Y, Wei P, Pengpumi S, Schumacher EA, Remcho VT (2015) Development of a carbon dot (C-Dot)-linked immunosorbent assay for the detection of human alpha-fetoprotein. *Anal Chem* 87(16):8510–8516. <https://doi.org/10.1021/acs.analchem.5b02019>
- Huang S, Yao J, Chu X, Liu Y, Xiao Q, Zhang Y (2019) One-step facile synthesis of nitrogen-doped carbon dots: a ratiometric fluorescent probe for evaluation of acetylcholinesterase activity and detection of organophosphorus pesticides in tap water and food. *J Agric Food Chem* 67(40):11244–11255. <https://doi.org/10.1021/acs.jafc.9b03624>
- Sajwan RK, Lakshmi G, Solanki PR (2021) Fluorescence tuning behavior of carbon quantum dots with gold nanoparticles via novel intercalation effect of aldicarb. *Food Chem* 340:127835. <https://doi.org/10.1016/j.foodchem.2020.127835>
- Kudr J, Richtera L, Xhaxhiu K, Hynek D, Heger Z, Zitka O, Adam V (2017) Carbon dots based FRET for the detection of DNA damage. *Biosens Bioelectron* 92:133–139. <https://doi.org/10.1016/j.bios.2017.01.067>
- Luo M, Wei J, Zhao Y, Sun Y, Liang H, Wang S, Li P (2020) Fluorescent and visual detection of methyl-paraoxon by using boron-and nitrogen-doped carbon dots. *Microchem J*. <https://doi.org/10.1016/j.microc.2019.104547>
- Gong P, Sun L, Wang F, Liu X, Yan Z, Wang M, Zhang L, Tian Z, Liu Z, You J (2019) Highly fluorescent N-doped carbon dots with two-photon emission for ultrasensitive detection of tumor marker and visual monitor anticancer drug loading and delivery. *Chem Eng J* 356:994–1002. <https://doi.org/10.1016/j.cej.2018.09.100>
- Zhang Y, Gao Z, Zhang W, Wang W, Chang J, Kai J (2018) Fluorescent carbon dots as nanoprobe for determination of lidocaine hydrochloride. *Sens Actuat B: Chem* 262:928–937. <https://doi.org/10.1016/j.snb.2018.02.079>
- Campos BB, Contreras-Cáceres R, Bandosz TJ, Jiménez-Jiménez J, Rodríguez-Castellón E, Esteves da Silva JCG, Algarra M (2016) Carbon dots as fluorescent sensor for detection of explosive nitro-compounds. *Carbon* 106:171–178. <https://doi.org/10.1016/j.carbon.2016.05.030>
- Yang Y, Ghalandari B, Lin L, Sang X, Su W, Divsalar A, Ding X (2022) A turn-on fluorescence sensor based on Cu(2+) modulated DNA-templated silver nanoclusters for glyphosate detection and mechanism investigation. *Food Chem* 367:130617. <https://doi.org/10.1016/j.foodchem.2021.130617>
- Guan J, Yang J, Zhang Y, Zhang X, Deng H, Xu J, Wang J, Yuan MS (2021) Employing a fluorescent and colorimetric picolyl-functionalized rhodamine for the detection of glyphosate pesticide. *Talanta* 224:121834. <https://doi.org/10.1016/j.talanta.2020.121834>
- Hou J, Dong J, Zhu H, Teng X, Ai S, Mang M (2015) A simple and sensitive fluorescent sensor for methyl parathion based on L-tyrosine methyl ester functionalized carbon dots. *Biosens Bioelectron* 68:20–26. <https://doi.org/10.1016/j.bios.2014.12.037>
- Gao Z, Wang L, Su R, Huang R, Qi W, He Z (2015) A carbon dot-based "off-on" fluorescent probe for highly selective and sensitive detection of phytic acid. *Biosens Bioelectron* 70:232–238. <https://doi.org/10.1016/j.bios.2015.03.043>
- Baig MMF, Chen YC (2017) Bright carbon dots as fluorescence sensing agents for bacteria and curcumin. *J Colloid Interface Sci* 501:341–349. <https://doi.org/10.1016/j.jcis.2017.04.045>
- Ding H, Du F, Liu P, Chen Z, Shen J (2015) DNA-carbon dots function as fluorescent vehicles for drug delivery. *ACS Appl Mater Interfaces* 7(12):6889–6897. <https://doi.org/10.1021/acsami.5b00628>
- Liu Z, Jin W, Wang F, Li T, Nie J, Xiao W, Zhang Q, Zhang Y (2019) Ratiometric fluorescent sensing of  $\text{Pb}^{2+}$  and  $\text{Hg}^{2+}$  with two types of carbon dot nanohybrids synthesized from the same biomass. *Sensors and Actuators B: Chemical*. <https://doi.org/10.1016/j.snb.2019.126698>
- Kumar VB, Kumar R, Gedanken A, Shefi O (2019) Fluorescent metal-doped carbon dots for neuronal manipulations. *Ultrason Sonochem* 52:205–213. <https://doi.org/10.1016/j.ultsonch.2018.11.017>
- Atchudan R, Edison T, Aseer KR, Perumal S, Karthik N, Lee YR (2018) Highly fluorescent nitrogen-doped carbon dots derived from *Phyllanthus acidus* utilized as a fluorescent probe for label-free selective detection of  $\text{Fe}^{3+}$  ions, live cell imaging and fluorescent ink. *Biosens Bioelectron* 99:303–311. <https://doi.org/10.1016/j.bios.2017.07.076>
- Shangguan J, Huang J, He D, He X, Wang K, Ye R, Yang X, Qing T, Tang J (2017) Highly  $\text{Fe}^{3+}$ -selective fluorescent nanoprobe based on ultrabright N/P codoped carbon dots and its application in biological samples. *Anal Chem* 89(14):7477–7484. <https://doi.org/10.1021/acs.analchem.7b01053>
- Liu W, Li C, Sun X, Pan W, Wang J (2017) Carbon-dot-based ratiometric fluorescent pH sensor for the detections of very weak acids assisted by auxiliary reagents that contribute to the release



- of protons. *Sensors and Actuators B: Chemical* 244:441–449. <https://doi.org/10.1016/j.snb.2017.01.009>
21. Liu C, Ning D, Zhang C, Liu Z, Zhang R, Zhao J, Zhao T, Liu B, Zhang Z (2017) Dual-colored carbon dot ratiometric fluorescent test paper based on a specific spectral energy transfer for semiquantitative assay of copper ions. *ACS Appl Mater Interfaces* 9(22):18897–18903. <https://doi.org/10.1021/acsami.7b05827>
  22. Wang M, Li M, Lu J, Fan B, He Y, Huang Y, Wang F (2018) “Off-On” fluorescent sensing of organophosphate pesticides using a carbon dot–Au(III) complex. *RSC Advances* 8(21):11551–11556. <https://doi.org/10.1039/c7ra13404e>
  23. Liu G, Zhao H, Diao F, Ling Z, Wang Y (2018) Stable tandem luminescent solar concentrators based on CdSe/CdS quantum dots and carbon dots. *J Mater Chem C* 6(37):10059–10066. <https://doi.org/10.1039/c8tc02532k>
  24. Li Y, Bi J, Liu S, Wang H, Yu C, Li D, Zhu BW, Tan M (2017) Presence and formation of fluorescence carbon dots in a grilled hamburger. *Food Funct* 8(7):2558–2565. <https://doi.org/10.1039/c7fo00675f>
  25. Guerrero-Esteban T, Gutiérrez-Sánchez C, Martínez-Periñán E, Revenga-Parra M, Pariente F, Lorenzo E (2021) Sensitive glyphosate electrochemiluminescence immunosensor based on electrografted carbon nanodots. *Sensors and Actuators B: Chemical*. <https://doi.org/10.1016/j.snb.2020.129389>
  26. Bera MK, Mohapatra S (2020) Ultrasensitive detection of glyphosate through effective photoelectron transfer between CdTe and chitosan derived carbon dot. *Colloids and Surfaces A: Physicochemical and Engineering Aspects*. <https://doi.org/10.1016/j.colsurfa.2020.124710>
  27. Jimenez-Lopez J, Llorent-Martinez EJ, Ortega-Barrales P, Ruiz-Medina A (2020) Graphene quantum dots-silver nanoparticles as a novel sensitive and selective luminescence probe for the detection of glyphosate in food samples. *Talanta* 207:120344. <https://doi.org/10.1016/j.talanta.2019.120344>
  28. Wang L, Bi Y, Hou J, Li H, Xu Y, Wang B, Ding H, Ding L (2016) Facile, green and clean one-step synthesis of carbon dots from wool: application as a sensor for glyphosate detection based on the inner filter effect. *Talanta* 160:268–275. <https://doi.org/10.1016/j.talanta.2016.07.020>
  29. Yuan Y, Jiang J, Liu S, Yang J, Zhang H, Yan J, Hu X (2017) Fluorescent carbon dots for glyphosate determination based on fluorescence resonance energy transfer and logic gate operation. *Sensors and Actuators B: Chemical* 242:545–553. <https://doi.org/10.1016/j.snb.2016.11.050>
  30. Wang L, Bi Y, Gao J, Li Y, Ding H, Ding L (2016) Carbon dots based turn-on fluorescent probes for the sensitive determination of glyphosate in environmental water samples. *RSC Advances* 6(89):85820–85828. <https://doi.org/10.1039/c6ra10115a>
  31. Wang D, Lin B, Cao Y, Guo M, Yu Y (2016) A highly selective and sensitive fluorescence detection method of glyphosate based on an immune reaction strategy of carbon dot labeled antibody and antigen magnetic beads. *J Agric Food Chem* 64(30):6042–6050. <https://doi.org/10.1021/acs.jafc.6b01088>
  32. Hou J, Wang X, Lan S, Zhang C, Hou C, He Q, Huo D (2020) A turn-on fluorescent sensor based on carbon dots from *Sophora japonica* leaves for the detection of glyphosate. *Anal Methods* 12(33):4130–4138. <https://doi.org/10.1039/d0ay01241f>
  33. Ashrafi Tafreshi F, Fatahi Z, Ghasemi SF, Taherian A, Esfandiari N (2020) Ultrasensitive fluorescent detection of pesticides in real sample by using green carbon dots. *PLoS One* 15(3):e0230646. <https://doi.org/10.1371/journal.pone.0230646>
  34. Hou J, Dong G, Tian Z, Lu J, Wang Q, Ai S, Wang M (2016) A sensitive fluorescent sensor for selective determination of dichlorvos based on the recovered fluorescence of carbon dots-Cu(II) system. *Food Chem* 202:81–87. <https://doi.org/10.1016/j.foodchem.2015.11.134>
  35. Xu XY, Yan B, Lian X (2018) Wearable glove sensor for non-invasive organophosphorus pesticide detection based on a double-signal fluorescence strategy. *Nanoscale* 10(28):13722–13729. <https://doi.org/10.1039/c8nr03352h>

**Publisher's note** Springer Nature remains neutral with regard to jurisdictional claims in published maps and institutional affiliations.